



BELLE2-CONF-PH-2021-012
June 29, 2022

Measurement of the inclusive semileptonic B meson branching fraction in 62.8 fb^{-1} of Belle II data

(The Belle II Collaboration)

Abstract

We report a measurement of the branching fraction of inclusive semileptonic B meson decays $B \rightarrow X_c \ell \nu_\ell$ in $\Upsilon(4S) \rightarrow B\bar{B}$ data recorded by the Belle II experiment at the SuperKEKB asymmetric-energy e^+e^- collider and corresponding to 62.8 fb^{-1} of integrated luminosity. Only a charged lepton (electron or muon) is reconstructed and the signal yield is determined from a fit to the lepton momentum distribution in the center-of-mass frame of the colliding beams. Averaging the result in the electron and muon channels, we find $\mathcal{B}(B \rightarrow X_c \ell \nu_\ell) = (9.75 \pm 0.03(\text{stat}) \pm 0.47(\text{sys}))\%$.

arXiv:2111.09405v1 [hep-ex] 17 Nov 2021

1. INTRODUCTION

The magnitude of the Cabibbo-Kobayashi-Maskawa (CKM) [1, 2] matrix element $|V_{cb}|$ squared determines the transition rate of b into c quarks. The precise knowledge of this fundamental parameter of the Standard Model (SM) [3] is crucial for the ongoing precision B physics programme at the Belle II experiment and elsewhere. The CKM element $|V_{cb}|$ is measured from semileptonic B meson decays $B \rightarrow X_c \ell \nu_\ell$, where X_c is a hadronic system with charm, ℓ is a light charged lepton (electron or muon) and ν is the associated neutrino. These determinations can be *inclusive*, *i.e.*, sensitive to all $X_c \ell \nu_\ell$ final states within a given region of phase space, or *exclusive*, *i.e.*, based only on a single $b \rightarrow c$ semileptonic mode such as $B \rightarrow D^* \ell \nu$ or $B \rightarrow D \ell \nu$. Pursuing both approaches is important as the two avenues involve different theoretical and experimental uncertainties and consistency between both is a powerful consistency check of our understanding. However, inclusive and exclusive measurements of $|V_{cb}|$ have been at odds for many years now, an issue which is often referred to as the *inclusive vs. exclusive problem* [4].

In this paper we describe a measurement of the inclusive semileptonic branching ratio based on the Belle II data collected in the years 2019 and 2020 equivalent to 62.8 fb^{-1} . The paper is organized as follows: Sect. 2 describes the collision data and simulated data samples used in this analysis. Sect. 3 introduces our experimental procedure. Finally, Sect. 4 contains all results and the analysis of systematic uncertainties.

2. THE BELLE II DETECTOR AND DATA SAMPLE

The Belle II detector [5] operates at the SuperKEKB asymmetric-energy electron-positron collider [6], located at the KEK laboratory in Tsukuba, Japan. The detector consists of several nested detector subsystems arranged around the beam pipe in a cylindrical geometry. The innermost subsystem is the vertex detector, which includes two layers of silicon pixel detectors and four outer layers of silicon strip detectors. Currently, the second pixel layer is installed in only a small part of the solid angle, while the remaining vertex detector layers are fully installed. Most of the tracking volume consists of a helium and ethane-based small-cell drift chamber (CDC). Outside the drift chamber, a Cherenkov-light imaging and time-of-propagation detector provides charged-particle identification in the barrel region. In the forward endcap, this function is provided by a proximity-focusing, ring-imaging Cherenkov detector with an aerogel radiator. Further out is the ECL electromagnetic calorimeter, consisting of a barrel and two endcap sections made of CsI(Tl) crystals. A uniform 1.5 T magnetic field is provided by a superconducting solenoid situated outside the calorimeter. Multiple layers of scintillators and resistive plate chambers, located between the magnetic flux-return iron plates, constitute the K_L and muon identification system (KLM).

The data used in this analysis were collected between March 2019 and July 2020 and correspond to 62.8 fb^{-1} of integrated luminosity on the $\Upsilon(4S)$ resonance (10.58 GeV) and 9.2 fb^{-1} of integrated luminosity below the $\Upsilon(4S)$ resonance (10.52 GeV), referred to as *off-resonance data*. Collected data sample contains $N_{B\bar{B}} = (68.21 \pm 0.06(\text{stat}) \pm 0.75(\text{sys})) \times 10^6$ $\Upsilon(4S) \rightarrow B\bar{B}$ events as determined from a fit to event-shape variables [7]. In addition, we use Monte Carlo (MC) simulated events equivalent to 200 fb^{-1} throughout this analysis. These include a sample of $\Upsilon(4S) \rightarrow B\bar{B}$ events in which B mesons decay generically, generated

with EvtGen [8] and a sample of continuum $e^+e^- \rightarrow q\bar{q}$ events ($q = u, d, s, c$) simulated with KKMC [9], interfaced with PYTHIA [10]. The $B\bar{B}$ sample includes semileptonic B meson decays $B \rightarrow X\ell\nu$, where X can be a hadronic system with and without charm. The latter is modeled by a mixture of exclusive modes (X_u can either be charged or neutral π, ρ, ω or η) and an inclusive model [11]. Full detector simulation based on GEANT4 [12] is applied to MC events. The lepton reconstruction efficiencies and the hadron misidentification rates in simulation are adjusted to match the real performance of the Belle II lepton identification system.

Both data and simulated events are analysed with Belle II analysis software framework (BASF2) [13]. Hadronic events are selected and backgrounds coming from quantum electrodynamic processes (low multiplicity events) are reduced by requiring more than three charged tracks in a single event, the total energy of the reconstructed charged and neutral particles above 4 GeV and a ratio R_2 of the second to the zeroth Fox-Wolfram moment below 0.4 [14].

3. EXPERIMENTAL PROCEDURE

3.1. Reconstruction

We require charged particle tracks to originate from the interaction point (IP): The distance of closest approach between each track and the interaction point is required to be less than 2 cm along the z direction (parallel to the beams) and less than 0.5 cm in the transverse $r - \phi$ plane. We further require charged particles to be within acceptance of the central drift chamber (CDC) and to have transverse momentum above 100 MeV/ c .

In the next step, we identify charged lepton candidates (electrons or muons). The particle's center-of-mass (c.m.) momentum p_ℓ^* must lie in the range between 0.4 and 2.5 GeV/ c . Electrons are identified based on their energy and shower shape in the ECL calorimeter. Muons are identified using information from the instrumented return yoke KLM. We require the lepton candidates to have momenta in the laboratory frame within the range of $p_\ell \in [0.4, 2.5]$ GeV/ c and polar angle $\theta_e \in [0.22, 2.71]$ rad for electrons and $\theta_\mu \in [0.4, 2.6]$ rad for muons. We veto charged leptons from J/ψ decays or from photon conversion. Each lepton candidate is combined with an oppositely charged particle and two regions of invariant mass $M(\ell^+\ell^-)$ are excluded – the interval $[3.0, 3.14]$ GeV/ c^2 for electrons and $[3.04, 3.14]$ GeV/ c^2 for muons. Photon conversions to an electron pair are vetoed by rejecting electron positron pairs with an invariant mass below 0.14 GeV. We also reject events with more than one lepton candidate.

We exclude events where the missing momentum is not consistent with the presence of a single neutrino from the semileptonic B decay. In particular we impose the event-level selections on the following three properties: missing mass (magnitude of the missing four-momentum) is required to be $M_{miss}^2 < 3$ GeV 2 , the polar angle of the missing three-momentum has to lie within $\theta_{miss} \in [0.3, 2.6]$ rad and the absolute value of the total event charge is restricted to $|\sum_i q_i| < 3$.

The MC samples are scaled to the data luminosity and split up into the following components: $B \rightarrow X_c\ell\nu_\ell$ signal, $B \rightarrow X_u\ell\nu_\ell$ background, the events where the lepton candidate

is misidentified (referred to as *fakes* or *fake leptons*), $b \rightarrow c/\bar{c} \rightarrow \ell$ (secondary leptons), and other $B\bar{B}$ background (the lepton candidate does not belong in any of these categories). The lepton identification at Belle II is described in [15].

3.2. Signal extraction

We extract the amount of $B \rightarrow X_c \ell \nu_\ell$ signal and background by performing a fit to the binned c.m. lepton momentum distribution, separately in the electron and in the muon samples. We use a maximum likelihood technique using Poisson statistics of both real and MC simulated data [16]. The following components are freely floated in this fit: the $b \rightarrow c$ signal, $B\bar{B}$ backgrounds (including $b \rightarrow u$, fake and secondary leptons and other $B\bar{B}$ backgrounds) and the continuum background. The shape in p_ℓ^* of the signal and $B\bar{B}$ backgrounds components are obtained from MC simulation, while the shape of the continuum background is modeled by off-resonance collision data equivalent to 9.2 fb^{-1} , taken at the c.m. energy of 10.52 GeV .

It is necessary to combine all $B\bar{B}$ background contributions into a single fit component because they have similar shapes in p_ℓ^* and the fit would otherwise have difficulties to distinguish them. However, we vary the relative amounts of these background components when evaluating the systematic uncertainty related to the background and repeat the fit with altered compositions of the background.

Fig. 1 shows the c.m. frame electron and muon momentum distributions after the fit. Table I gives the yields of the various components and their respective uncertainties determined by the fit.

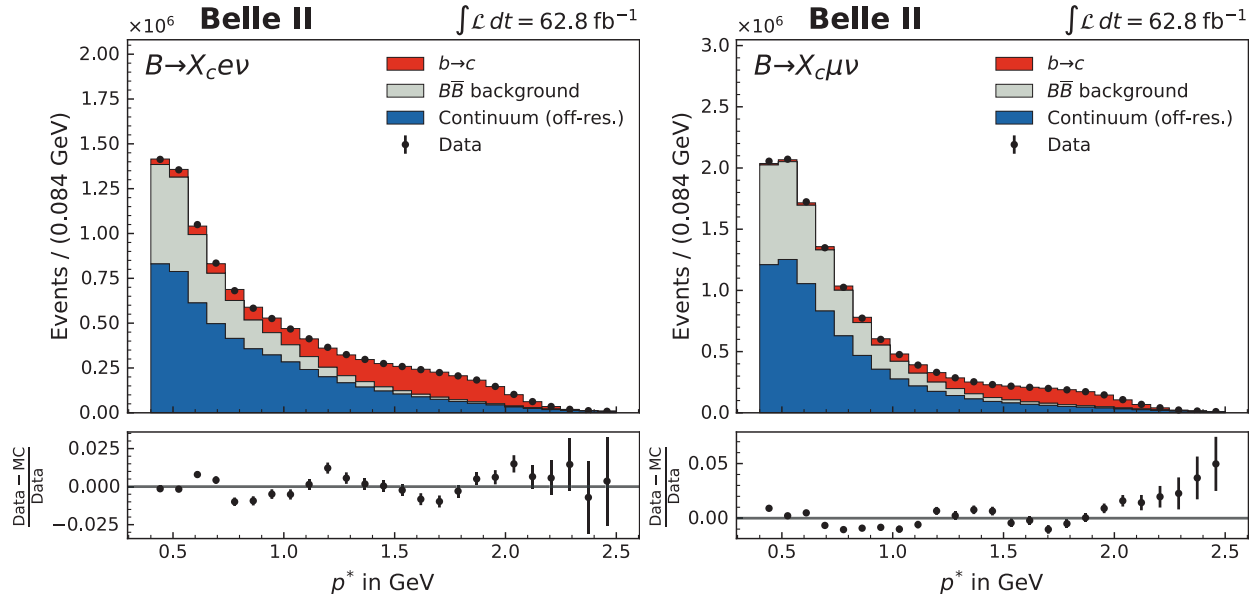


FIG. 1. C.m. frame electron (left) and muon (right) momentum distributions after the fit. See text for more details.

TABLE I. Yields in the electron and muon samples. Note that the $b \rightarrow u$, fake and secondary leptons and other $B\bar{B}$ background components are combined in a single fit component and that they are split up here for better understanding. See text for more details.

Yield	Electron mode	Muon mode
Signal	$(1.932 \pm 0.006) \times 10^6$	$(1.501 \pm 0.007) \times 10^6$
$b \rightarrow u$ background	$(53.4 \pm 0.4) \times 10^3$	$(52 \pm 1) \times 10^3$
Fake leptons	$(1.258 \pm 0.009) \times 10^6$	$(3.15 \pm 0.07) \times 10^6$
Secondaries	$(1.324 \pm 0.009) \times 10^6$	$(0.89 \pm 0.02) \times 10^6$
Other $B\bar{B}$ background	$(5.42 \pm 0.04) \times 10^3$	$(4.33 \pm 0.09) \times 10^3$
Continuum	$(5.51 \pm 0.02) \times 10^6$	$(7.35 \pm 0.09) \times 10^6$
Sum	$(10.08 \pm 0.03) \times 10^6$	$(13.0 \pm 0.1) \times 10^6$

4. RESULTS AND SYSTEMATIC UNCERTAINTIES

4.1. Inclusive semileptonic branching fraction

In this section we determine the inclusive branching fraction of semileptonic decays $B \rightarrow X_c \ell \nu_\ell$ where B is a state with the average lifetime of B^+ and B^0 , $\tau = (\tau(B^+) + \tau(B^0))/2 = (1.579 \pm 0.004)$ ps [17]. As spectator effects in semileptonic decays are known to be small [18], we assume a common semileptonic width

$$\Gamma_{\text{s.l.}} = \frac{\mathcal{B}(B^+ \rightarrow X_c \ell \nu_\ell)}{\tau(B^+)} = \frac{\mathcal{B}(B^0 \rightarrow X_c \ell \nu_\ell)}{\tau(B^0)} = \frac{\mathcal{B}(B \rightarrow X_c \ell \nu_\ell)}{\tau}, \quad (1)$$

and calculate the inclusive semileptonic branching fraction as

$$\mathcal{B}(B \rightarrow X_c \ell \nu_\ell) = \frac{N_{\text{sig}}^\ell \tau}{2N_{B\bar{B}} \left(f_+ \epsilon^\ell(B^+) \tau(B^+) + f_0 \epsilon^\ell(B^0) \tau(B^0) \right)}, \quad (2)$$

where N_{sig}^ℓ is the fitted number of signal events in the respective sample, $N_{B\bar{B}}$ is the total number of $B\bar{B}$ pairs in the data sample and $\epsilon^\ell(B)$ is the signal selection efficiency in the respective sample. The factor of two accounts for the fact that both B mesons in the $\Upsilon(4S)$ event can contribute to the signal. The factors $\tau(B^+/B^0)$ are the mean lifetimes of the mesons and the $f_{+/0}$ are the production fractions of the two B species at the $\Upsilon(4S)$. We determine them from $f_+/f_0 = 1.058 \pm 0.024$ [17] to be $f_+ = 0.514 \pm 0.006$ and $f_0 = 0.486 \pm 0.006$.

The signal selection efficiencies were determined from MC simulation for the B^+ and B^0 events separately. The electron mode efficiencies after all applied selections are $\epsilon^e(B^+) = 15.76\%$ and $\epsilon^e(B^0) = 12.40\%$. The muon mode has somewhat lower signal selection efficiencies of $\epsilon^\mu(B^+) = 12.99\%$ and $\epsilon^\mu(B^0) = 10.03\%$.

From this equation we obtain the following branching fractions in the electron and muon samples. The uncertainty is statistical only, *i.e.*, corresponds to the uncertainty in the fitted

signal fraction.

$$\mathcal{B}(B \rightarrow X_c e \nu_e) = (9.97 \pm 0.03(\text{stat}))\% , \quad (3)$$

$$\mathcal{B}(B \rightarrow X_c \mu \nu_\mu) = (9.47 \pm 0.05(\text{stat}))\% . \quad (4)$$

4.2. Systematic Uncertainties

The main contribution is model uncertainty in the $B \rightarrow X_c \ell \nu_\ell$ signal and in the $B\bar{B}$ background component. The $B \rightarrow X_c \ell \nu_\ell$ modelling uncertainty in Monte Carlo was determined in the following way: At first, the inclusive signal sample was split into 30 separate decay modes. The branching fraction of the mode under consideration was varied by $\pm 1\sigma$ of the current average branching fraction, taken from the Particle Data Group [17]. The whole sample was then fitted again and the number of signal events was obtained from the fit. The systematic uncertainty was calculated for each decay mode from the difference between maximal and minimal yield, and the true signal yield from Table I. The full modeling uncertainty is calculated by adding the separate contributions in quadrature.

The decay form factors affect the shape of the Monte Carlo template in center-of-mass (c.m.) momentum p_ℓ^* . The form factor uncertainty is estimated by assuming the Caprini, Lellouch and Neubert (CLN) parameterization [19] for the $B \rightarrow D^* \ell \nu_\ell$ and $B \rightarrow D \ell \nu_\ell$ decays and varying the form factor parameters within their ranges of uncertainty [4].

To estimate the uncertainty in the $B\bar{B}$ background, we vary all four contributions ($b \rightarrow u$, secondary leptons, fake leptons and others) by 5%, which roughly corresponds to the difference between pre-fit and post-fit yields of the background. We determine uncertainties in the same way as for the $B \rightarrow X_c \ell \nu_\ell$ model. Furthermore, we constrain continuum background to the ratio between on- and off-resonance data of $62.8 \text{ fb}^{-1}/9.2 \text{ fb}^{-1}$, allowing it to float only within the uncertainty of the luminosity measurement (later referred to as ‘fixed’ continuum ratio). The uncertainty assigned to the continuum background is the difference between yields with ‘fixed’ and fully floating fraction in the fit. Details on the determination of the background model uncertainty are collected in Table II.

TABLE II. Determination of the background model uncertainty. The table shows the change in fitted signal yield when varying individual background components by $\pm 5\%$.

Varying background	Electron mode			Muon mode		
	$N_{sig,0.95}$	$N_{sig,1.05}$	σ_{rel} [%]	$N_{sig,0.95}$	$N_{sig,1.05}$	σ_{rel} [%]
$b \rightarrow u$	1934639	1928820	0.15	1505782	1509395	0.12
Fake leptons	1930435	1928590	0.05	1519457	1511576	0.26
Secondaries	1927430	1934593	0.19	1506999	1508290	0.04
Others	1932781	1932126	0.02	1508798	1503859	0.16
Continuum data (‘fixed’ ratio)	1925908		0.34	1457793		2.91

Other components are uncertainties related to tracking, to the counting of $B\bar{B}$ events and to lepton identification. The uncertainty related to lepton identification is estimated by generating 200 variations of the simulated events with lepton identification efficiency

and misidentification rates chosen randomly within their respective uncertainties. For each variation, the number of signal events ($N_{sig,i}$) is calculated. The mean value and the standard deviation of the distribution of the obtained yields $N_{sig,i}$ are used to determine the lepton identification uncertainty.

A tracking uncertainty of 0.69% is applied to the only charged particle that is reconstructed. The uncertainty from limited MC sample size in the reconstruction efficiency $\epsilon^\ell(B)$ is at the sub-permille level and therefore negligible. Table III summarizes our estimate of the systematic uncertainty in the electron and muon samples. The different components of systematic uncertainty are added in quadrature and the overall relative systematic uncertainties are found to be 3.77% and 4.79% for the electron and muon modes, respectively.

TABLE III. Estimated relative systematic uncertainty on the $B \rightarrow X_c \ell \nu_\ell$ branching fraction measurement in the two modes.

Contribution	Relative uncertainty [%]	
	Electron mode	Muon mode
Tracking	0.69	0.69
$N_{B\bar{B}}$	1.1	1.1
Lepton ID corrections	1.64	2.33
f_0/f_+ , B lifetime	1.2	1.2
$B \rightarrow X_c \ell \nu_\ell$ branching fractions	2.65	2.15
$B \rightarrow X_c \ell \nu_\ell$ form factors	1.11	1.11
$B\bar{B}$ background model	0.24	0.34
Off-resonance data model	0.34	2.91
Sum	3.77	4.79

5. CONCLUSION

We have measured the inclusive $B \rightarrow X_c \ell \nu_\ell$ branching ratio in a Belle II sample corresponding to 62.8 fb^{-1} of integrated luminosity. The preliminary results for both lepton modes are

$$\mathcal{B}(B \rightarrow X_c e \nu_e) = (9.97 \pm 0.03(\text{stat}) \pm 0.38(\text{sys}))\% , \quad (5)$$

$$\mathcal{B}(B \rightarrow X_c \mu \nu_\mu) = (9.47 \pm 0.05(\text{stat}) \pm 0.45(\text{sys}))\% . \quad (6)$$

The combined branching fraction is determined as the weighted mean. We conservatively assume electron and muon systematic uncertainties to be fully correlated and use the (larger) muon systematic uncertainty for the combined result. The average semileptonic branching fraction $B \rightarrow X_c \ell \nu_\ell$ (where ℓ can be either an electron or a muon) is thus found to be

$$\mathcal{B}(B \rightarrow X_c \ell \nu_\ell) = (9.75 \pm 0.03(\text{stat}) \pm 0.47(\text{sys}))\% . \quad (7)$$

-
- [1] N. Cabibbo, *Phys. Rev. Lett.* **10**, 531 (1963).
 - [2] M. Kobayashi and T. Maskawa, *Prog. Theor. Phys.* **49**, 652 (1973).
 - [3] A. Pich, in *2006 European School of High-Energy Physics* (2008) pp. 1–49, arXiv:0705.4264 [hep-ph].
 - [4] Y. S. Amhis *et al.* (HFLAV), (2019), arXiv:1909.12524 [hep-ex].
 - [5] T. Abe *et al.* (Belle II Collaboration), (2010), arXiv:1011.0352 [physics.ins-det].
 - [6] Y. Ohnishi *et al.*, *PTEP* **2013**, 03A011 (2013).
 - [7] F. Abudinén *et al.* (Belle II Collaboration), BELLE2-NOTE-PL-2020-006.
 - [8] D. J. Lange, *Nucl. Instrum. Meth.* **A462**, 152 (2001).
 - [9] S. Jadach, B. F. L. Ward, and Z. Was, *Comput. Phys. Commun.* **130**, 260 (2000).
 - [10] T. Sjostrand, S. Mrenna, and P. Z. Skands, *Comput. Phys. Commun.* **178**, 852 (2008), arXiv:0710.3820 [hep-ph].
 - [11] F. D. Fazio and M. Neubert, *Journal of High Energy Physics* **1999**, 017–017 (1999), arXiv:hep-ph/9905351 [hep-ph].
 - [12] S. Agostinelli *et al.* (GEANT4 Collaboration), *Nucl. Instrum. Meth.* **A506**, 250 (2003).
 - [13] T. Kuhr, C. Pulvermacher, M. Ritter, T. Hauth, and N. Braun (Belle-II Framework Software Group), *Comput. Softw. Big Sci.* **3**, 1 (2019), arXiv:1809.04299 [physics.comp-ph].
 - [14] G. C. Fox and S. Wolfram, *Phys. Rev. Lett.* **41**, 1581 (1978).
 - [15] M. Milesi, J. Tan, and P. Urquijo, *EPJ Web of Conferences* **245**, 06023 (2020).
 - [16] R. J. Barlow and C. Beeston, *Comput. Phys. Commun.* **77**, 219 (1993).
 - [17] P. Zyla *et al.* (Particle Data Group), *PTEP* **2020**, 083C01 (2020).
 - [18] M. Di Pierro and C. T. Sachrajda (UKQCD), *Nucl. Phys. B* **534**, 373 (1998), arXiv:hep-lat/9805028.
 - [19] I. Caprini, L. Lellouch, and M. Neubert, *Nucl. Phys. B* **530**, 153 (1998), arXiv:hep-ph/9712417.